Failure of dietary quercetin to alter the temporal progression of insulin resistance among tissues of C57BL/6J mice during the development of diet-induced obesity

L. K. Stewart[1], **Z. Wang**[2], **D. Ribnicky**[3], **J. L. Soileau**[1], **W. T. Cefalu**[2], and **T. W. Gettys**[1]

[1] Laboratory of Nutrient Sensing and Adipocyte Signaling, Pennington Biomedical Research Center, 6400 Perkins Road, Baton Rouge, LA 70808, USA, e-mail: gettystw@pbrc.edu

[2] Center for the Study of Botanicals and Metabolic Syndrome, Pennington Biomedical Research Center, Baton Rouge, LA, USA

[3] Biotech Center-Rutgers University, New Brunswick, NJ, USA

Abstract

Aims/hypotheses—High-fat diets produce obesity and glucose intolerance by promoting the development of insulin resistance in peripheral tissues and liver. The present studies sought to identify the initial site(s) where insulin resistance develops using a moderately high-fat diet and to assess whether the bioflavonoid, quercetin, ameliorates progression of this sequence.

Methods—Four cohorts of male C57BL/6J mice were placed on diets formulated to be low-fat (10% of energy from fat), high-fat (45% of energy from fat) or high-fat plus 1.2% quercetin (wt/wt). After 3 and 8 weeks, cohorts were evaluated using euglycaemic–hyperinsulinaemic clamps, metabolomic analysis of fatty acylcarnitines and acute in vitro assessments of insulin signalling among tissues.

Results—After 3 and 8 weeks, the high-fat diet produced whole-body insulin resistance without altering insulin-dependent glucose uptake in peripheral tissues. The primary defect was impaired suppression of hepatic glucose production by insulin at both times. Quercetin initially exacerbated the effect of high-fat diet by further increasing hepatic insulin resistance, but by 8 weeks insulin resistance and hepatic responsiveness to insulin were similarly compromised in both high-fat groups. The high-fat diet, irrespective of quercetin, increased short-chain fatty acylcarnitines in liver but not in muscle, while reciprocally reducing hepatic long-chain fatty acylcarnitines and increasing them in muscle.

Conclusions/interpretation—Failure of insulin to suppress hepatic glucose output is the initial defect that accounts for the insulin resistance that develops after short-term consumption of a high-fat (45% of energy) diet. Hepatic insulin resistance is associated with accumulation of short- and medium-, but not long-chain fatty acylcarnitines. Dietary quercetin does not ameliorate the progression of this sequence.

Keywords

Adipose tissue; Botanicals; Euglycaemic-hyperinsulinaemic clamp; Glucose uptake; Hepatic glucose production; Insulin resistance

Introduction

Type 2 diabetes occurs when the pancreas cannot compensate fully for insulin resistance in peripheral tissues. Insulin resistance is strongly linked to development of obesity, but the complex events that occur in multiple organs and lead to diabetes remain poorly understood. The fat-sensitive C57BL/6J mouse has emerged as a key model to study the developmental pathology of the obese/diabetic syndrome produced by chronic consumption of high-fat (HF) diets [1]. It remains unclear whether the initial stages of insulin resistance are the product of a uniform progression of insulin resistance across tissues or the result of a sequential but punctuated progression of insulin resistance among tissues. This lack of consensus is probably due to a combination of differences in the amount, source and saturation of dietary fat, as well as animal age and duration of exposure prior to evaluation of insulin resistance [2–6].

Quercetin, a bioflavonoid abundant in apples, onions and tea, is a dietary antioxidant associated with improved antioxidant status [7], lower incidence of ischaemic heart disease [8], delayed progression of atherosclerosis in apolipoprotein E-null mice [9] and increased ratio of oxidised to reduced glutathione in mice [9]. Quercetin also protected against oxidative damage in isolated mitochondria [10], macrophages [11] and cardiomyoblasts [12]. Recent reports [13, 14] show that dietary quercetin reduced circulating markers of inflammation and ameliorated components of metabolic syndrome in genetic and diet-induced models of obesity. Given the emerging consensus that mitochondrial dysfunction, inflammation, disordered lipid metabolism and reactive oxygen species are associated with the development of insulin resistance and diabetes [15–18], we sought here to determine whether dietary quercetin could ameliorate the progression of insulin resistance in C57BL/6J mice consuming a moderately HF diet.

Growing evidence indicates that lipid accumulation in tissues not designed for storage is directly involved in development of insulin resistance [16,19,20]. Incomplete mitochondrial oxidation of fatty acids may be an underlying mechanism, so we also sought to determine whether dietary quercetin could ameliorate the progression of diet-induced insulin resistance and modify mitochondrial lipid catabolism. Using longitudinal studies and state-of-the art in vivo and in vitro approaches, we show that diet-induced insulin resistance begins in the liver, is associated with hepatic accumulation of short- to medium-, but not long-chain fatty acylcarnitines, and is not ameliorated by dietary quercetin.

Methods

Animals and diets

Male 6-week-old C57BL/6J mice from Jackson Laboratory (Bar Harbor, ME, USA) were randomly assigned to the following diets (Research Diets, New Brunswick, NJ, USA): (1) LF, (10% of energy from fat; D12450B); (2) HF (45% of energy from fat; D12451); or (3) HF + quercetin (HF+Q) (45% of energy from fat + 1.2% quercetin [wt/wt]; D06081502). All diets contained soya-bean oil (25 g/kg diet). The LF diet (16.12 kJ/g) contained 20 g lard/kg diet while both HF diets (19.80 kJ/g) contained 178 g lard/kg diet. Quercetin (≥98%; Sigma, St Louis, MO, USA) was added to the HF+Q diet by cold processing. Diets were stored at 4°C in light-protected, airtight containers. Food was changed every 3 days, with free access to water. Mice were singly housed in shoebox cages with corncob bedding at 22°C on a 12 h light–dark

cycle. Food consumption was monitored weekly over 48 h. Experiments were approved by the Pennington Institutional Animal Care and Use Committee and conducted in facilities and using procedures that were consistent with the recommendations of the National Research Council's Guide for the Care and Use of Laboratory Animals, the Animal Welfare Act, and Public Health Service Policy on the Humane Care and Use of Laboratory Animals.

Studies were conducted with four cohorts of mice to evaluate in vivo and in vitro responses to diets. In cohort 1, food consumption and body composition were monitored for 8 weeks, followed by killing 16 mice per group at the peak (01:00 hours) and 16 mice per group at the nadir (13:00 hours) of the metabolic cycle. Liver and muscle were used to analyse fatty acylcarnitines and tissue triacylglycerol. Blood was obtained from 16 additional mice per group killed at time-points as above of the metabolic cycle. Insulin resistance was assessed in mice from cohort 2 with euglycaemic–hyperinsulinaemic clamps after 3 or 8 weeks on the diets. Acute signalling responses to insulin in liver and muscle were evaluated after an 8 h fast in cohort 3. In vitro responses to insulin were measured in adipocytes isolated from mice in cohort 4 after 8 weeks of diet.

Materials and reagents

Anti-Akt, anti-phosphoinositol 3-kinase (PI-3K) and anti-IRS1 were from UBI (Lake Placid, NY, USA). All other reagents were from Sigma. Kits for measuring plasma NEFA and triacylglycerol were from ZenBio (Research Triangle Park, NC, USA). Integrity of quercetin in the HF+Q diet and circulating quercetin were measured by mass spectrometry [13].

Metabolomic analysis

At 8 weeks, quadriceps muscle and liver were removed from mice in cohort 1, snap-frozen and extracts prepared for analysis of 45 fatty acylcarnitines by tandem mass spectrometry at the Stedman Nutrition and Metabolism Center at Duke Medical Center [21].

Euglycaemic–hyperinsulinaemic clamp

Mice were weaned on to respective diets at 6 weeks and in vivo insulin sensitivity was assessed after 3 and 8 weeks by the Vanderbilt Mouse Metabolic Phenotyping Center (Vanderbilt University School of Medicine, Nashville, TN, USA). Whole-body insulin sensitivity, tissue-specific glucose uptake and hepatic glucose production (Endo R_a) were determined using euglycaemic–hyperinsulinaemic clamps as described previously [22]. Arterial catheters were placed 5 days before the procedure and mice were fasted for 5 h before clamps.

Insulin signalling in muscle and liver

After 8 weeks on diets, mice in cohort 3 were fasted for 8 h and killed at baseline or 15 and 30 min post insulin injection (5 U/kg body weight). Liver and muscle samples were removed and snap-frozen. In whole-cell extracts from each tissue, PI-3K, Akt-1, Akt-2 and Akt-P (S-473) were analysed by western blot and IRS-1-associated PI-3K activity was measured in immunoprecipitates as described previously [23].

Acute insulin signalling in adipocytes

After 8 weeks, white adipocytes were isolated from mice in cohort 4 and preincubated with vehicle or 1 nmol/l insulin for 5 min at 37°C before addition of half log increments of isoproterenol from 1 to 1,000 nmol/l. After 60 min, inhibition of lipolysis by insulin was assessed by measuring glycerol release as described [24]. The experiment was repeated three times using three mice per diet for each replication.

Statistical analysis

Group means for food consumption, body composition, tissue acylcarnitines, plasma quercetin (cohort 1), euglycaemic–hyperinsulinaemic clamp variables (cohort 2) and variables from insulin signalling experiments (cohorts 3, 4) were analysed within each time point (3 or 8 weeks) by one-way ANOVA using animal within dietary treatment group as the error term [5]. Post hoc testing of group means within each time point was made with the Bonferroni correction using the pooled error term to calculate standard errors. In cohort 4, dose–response curves for isoproterenol-induced activation of lipolysis were compared using nonlinear least squares analysis [5]. For all contrasts, protection against type 1 errors was set at 5% (α=0.05).

Results

Food intake, body weight and body composition (cohort 1)

Energy intake did not differ among groups during the 1st week, but was 14% and 8% higher in the HF than the LF group at 3 and 8 weeks, respectively (p<0.05) (Table 1). The HF diet also affected nutrient partitioning, as evidenced by higher adiposity at 3 and 8 weeks in this group than in the LF group (p<0.05) (Table 1). Inclusion of quercetin did not affect energy intake, body weight or accretion of fat and protein at either time point (Table 1).

Euglycaemic–hyperinsulinaemic clamp (cohort 2)

In blood samples taken after a 5 h fast, blood glucose and plasma insulin were similar among the groups after 3 weeks of diet (Table 1). Blood glucose did not differ after 8 weeks, but fasting insulin was higher (p<0.05) in the HF than the LF group (Table 1). In contrast, fasting insulin in the HF+Q group was similar to the LF group and lower (p<0.05) than the HF group at 8 weeks (Table 1). At 8, but not 3 weeks, plasma NEFA was higher in the HF than the LF group (p< 0.05), while the HF+Q group was intermediate to both (Table 1). Plasma triacylglycerol levels were similarly ranked but did not differ among the groups at 3 or 8 weeks (Table 1). After 3 weeks, the glucose infusion rate (GIR) required to maintain euglycaemia was 24% lower in mice on the HF (0.211±0.011 mmol kg^{-1} min^{-1}) vs LF diet (0.262±0.011 mmol kg^{-1} min^{-1}) (Fig. 1a). At 8 weeks, another reduction of GIR in the HF group to 0.182± 0.019 mmol kg^{-1} min^{-1} was observed, consistent with further loss of insulin sensitivity. In contrast, GIR in the LF group was relatively unchanged (0.276±0.017 mmol kg^{-1} min^{-1}) between 3 and 8 weeks. The addition of quercetin to the HF diet did not ameliorate the reduction in GIR, but did exacerbate the insulin resistance produced by the HF diet at 3 weeks, such that the GIR was significantly lower (p<0.05) than the HF group (Fig. 1a). However, between 3 and 8 weeks, the GIR in the HF+Q group improved slightly, no longer differing from the HF group (Fig. 1b).

Tissue-specific uptake of 2-deoxy[^{14}C]glucose was highest in heart, followed by diaphragm, soleus, gastrocnemius, vastus lateralis muscle and white adipose tissue (Table 2). Interestingly, 2-deoxy[^{14}C]glucose uptake did not differ in any of the tissues at 3 or 8 weeks (Table 2). Basal endogenous hepatic glucose production (Endo R_a) was similar between LF and HF groups at 3 and 8 weeks, but insulin suppression of Endo R_a was impaired in the latter at both time points (Fig. 2a, b). Insulin did not suppress Endo R_a in the HF+Q group at 3 weeks (Fig. 2a), consistent with the reduction in GIR compared with the HF group (Fig. 1a). Insulin's ability to suppress Endo R_a was modestly restored at 8 weeks in the HF+Q group (Fig. 2b), although basal Endo R_a was also reduced in this group at 8 weeks (p<0.05).

Quercetin diet composition, absorption and degradation

Given the changes in insulin resistance in the HF+Q group, it was important to determine the stability of quercetin in the diet and examine circulating quercetin levels in the animals. The

HF+Q diet was formulated to contain 1.2% quercetin (wt/wt), but analysis after manufacture revealed 0.8% (wt/wt). The concentration was unchanged after 8 weeks of storage (~1% decrease). We therefore examined in vivo mechanisms and because food intake varies diurnally, plasma quercetin was measured in samples taken when food consumption is highest (01:00 hours) and lowest (13:00 hours). At 3 weeks, plasma quercetin varied diurnally between day (8 μg/ml) and night (12 μg/ml) as expected, with a similar variation between day (3 μg/ml) and night (7 μg/ml) seen at 8 weeks. Given no change in food intake or quercetin stability during this period, the twofold lower plasma quercetin during the day and 40% lower plasma quercetin at night between 8 and 3 weeks suggest an in vivo adaptive response. The data are consistent with a pharmacokinetic mechanism involving decreased absorption, enhanced degradation, increased excretion or some combination of these.

Metabolomic analysis of fatty acylcarnitines and tissue triacylglycerol

To test whether clamp-detected insulin resistance coincided with specific alterations in fatty acid catabolism profiles in liver and muscle, 45 acylcarnitines ranging in size (two to 22 carbons) and saturation were evaluated [21] after 8 weeks on the respective diets. In liver, 35 of the 45 acylcarnitines were unaffected by diet (Electronic supplementary material [ESM] Table 1, with a key to abbreviations in ESM Table 3). Of the remaining ten, four short-chain metabolites ranging from C4 to C8 were increased ($p<0.05$) by the HF relative to the LF diet (Fig. 3a); quercetin in the HF diet did not modify the increase in these metabolites. Two medium-chain acylcarnitines were higher ($p≤0.05$) in HF than LF (Fig. 3b), but were not increased by HF+Q relative to LF (Fig. 3b). In contrast, four long-chain metabolites (C14–C16) were significantly lower in the two HF groups than in the LF group (Fig. 3b). The acylcarnitine profiles in muscle were completely different, with only three of the 45 lipid metabolites altered by diet (ESM Table 2, with a key to abbreviations in ESM Table 3). The three that changed were all long-chain species (C16–C18) that were increased by the HF relative to the LF diet (Fig. 4). The response of these three acylcarnitines in the HF+Q group was indistinguishable from the HF group (Fig. 4).

Total hepatic triacylglycerol levels did not differ among the groups at 3 or 8 weeks (Table 1), but in muscle the HF and HF+Q groups had similar and higher triacylglycerol ($p<0.05$) than the LF group at 8 but not 3 weeks (Table 1). Collectively, the catabolic profiles suggest differential responses between the tissues. The simultaneous reduction of long-chain and accumulation of short-chain acylcarnitines is most consistent with enhanced but incomplete hepatic fatty acid catabolism in the HF groups. In muscle, the accumulation of long-chain acylcarnitines in the HF groups suggests some combination of increased uptake or decreased catabolism of fatty acids.

Insulin signalling in liver and muscle

Hepatic PI-3K level was unaffected by diet (Fig. 5a), but basal PI-3K activity was higher ($p<0.05$) in the HF and HF+Q groups than in the LF group (Fig. 5a). Insulin increased PI-3K activity 1.5-fold above basal in the HF group but produced no detectable activation above basal in HF+Q (Fig. 5b). In the LF group, insulin produced a 1.5- and 2.6-fold activation of PI-3K at 15 and 30 min (Fig. 5b). Basal Akt phosphorylation was higher in the two HF groups than the LF group (Fig. 5c), and higher in the HF+Q than in the HF group. In the two HF groups, insulin produced no additional activation of Akt; in the LF group it produced a 2.5-fold activation of Akt (Fig. 5d). The diets had no effect on hepatic protein content for GLUT2, IRS-1, IRS-2 or insulin receptor beta (data not shown).

In muscle, insulin produced comparable increases in PI-3K activity among the groups (Fig. 5e & f). In contrast, basal Akt phosphorylation was two- to threefold higher in the HF group compared with the LF and HF+Q groups. Despite higher basal Akt in the HF group, insulin

produced comparable additional activation of Akt among the groups (Fig. 5g, h). As in liver, production of many signalling intermediates did not differ among the groups (IRS-1, IRS-2, GLUT4, insulin receptor beta, AS160 and LAR).

Insulin signalling in adipocytes

To examine acute responsiveness of adipose tissue to insulin, the integrity of insulin signalling to type 3B phosphodiesterase was assessed by measuring insulin inhibition of cAMP-dependent lipolysis in adipocytes isolated from mice after 8 weeks on LF or HF diet. Figure 6 shows that isoproterenol produced comparable lipolytic responses in adipocytes from mice fed LF (EC_{50} =10.5±2.1 nmol/l) vs HF (EC_{50} =6.9±1.3 nmol/l) diets and that insulin produced a comparable decrease in isoproterenol EC_{50} between the two groups (LF =133±26; HF =89±21 nmol/l). This shows that inhibition of lipolysis by insulin was fully functional and not compromised by the HF diet.

Discussion

Accumulation of lipid in tissues not designed for storage is a key step in the initiation and progression of insulin resistance to diabetes [20,25,26]. The defective triacylglycerol storage in adipose tissue that occurs with lipodys-trophy results in rapid accumulation of lipid in liver and muscle. Ectopic fat deposition also occurs after chronic consumption of HF diets and is temporally related to periods of rapid weight gain and decreased insulin sensitivity [1,3,27]. An important unresolved question is whether the initial stage of insulin resistance is the product of uniform development of insulin resistance across tissues or the result of a sequential but punctuated progression of insulin resistance among specific tissues. Recent evidence suggests that mitochondrial lipid overload and incomplete fatty acid oxidation may compromise insulin sensitivity in muscle by increasing lipotoxic short-chain lipid metabolites that impair mitochondrial function [21,28–30]. The concept of lipid-induced mitochondrial dysfunction was developed in muscle, but it is unclear whether a similar mechanism is associated with development of insulin resistance in non-muscle sites. The present work addressed these issues using a combination of in vivo and in vitro approaches in longitudinal studies of C57BL/6J mice weaned on to a lard-based HF diet (45% energy from fat), with quercetin provided as a food admixture. The four major findings were: (1) whole-body insulin resistance was detected after 3 and 8 weeks on the HF diet and was entirely due to an inability of insulin to suppress endogenous glucose production from the liver; (2) muscle, adipose tissue and all other peripheral tissues retained full insulin sensitivity; (3) hepatic insulin resistance was associated with accumulation of short- to medium-chain and depletion of long-chain fatty acylcarnitines; and (4) dietary quercetin provided as a 0.8% (wt/wt) food admixture did not ameliorate diet-induced insulin resistance in this model.

The strong relationship between obesity and diabetes is well documented, but the mechanisms linking obesity to insulin resistance are less well understood. This is tied to the chronic nature of both conditions and the progressive deterioration in function of multiple, highly integrated organ systems that work together to maintain glucose homeostasis. The early recognition that C57BL/6J mice developed an obese/diabetic syndrome after consumption of a diet high in saturated fat established the C57BL/6J mouse as an important model for study of developmental progression of obesity and diabetes [1]. The initial design of weaning C57BL/6J mice on to a coconut oil-based HF diet (58% energy from fat) has been modified to use different amounts (58 vs 45% energy) and sources of fat, and introduce the diet at different ages. The approach has been extended to various rat lines that respond similarly and develop varying degrees of insulin resistance. Although few of these studies used longitudinal approaches and in vivo measurements (euglycaemic–hyperinsulinaemic clamps) to identify where insulin resistance first develops, the consensus is that very-HF diet formulations (55–

60% energy from fat) produce rapid deterioration in whole-body insulin sensitivity coincident with the appearance of hepatic and peripheral insulin resistance. The response pattern is common to rats and mice on very-HF diets, and supports the view that whole-body insulin resistance is the product of uniform progression of insulin resistance among peripheral tissues [3,4,31,32]. However, with a slightly lower percentage of dietary fat (45% of energy), compromised suppression of hepatic glucose production by insulin may be the primary initial cause of whole-body insulin resistance, followed by progressive loss of insulin-sensitive glucose uptake in peripheral tissues. Our findings indicate that mild whole-body insulin resistance after 3 weeks on the HF diet (45% of energy from fat) was due solely to failure of insulin to suppress Endo R_a without any change in insulin-dependent glucose uptake in peripheral tissues. And although whole-body insulin resistance increased after 8 weeks on the HF diet, it was still entirely accounted for by a corresponding loss of suppression of hepatic Endo R_a by insulin. The integrity of the initial steps of insulin signalling was assessed in mice killed at 0, 15 and 30 min after acute injection with insulin. These findings paralleled the in vivo data and show that insulin-dependent activation of Akt and PI-3K were compromised in liver but not muscle after 8 weeks on the HF diet. Together, these findings indicate that the insulin resistance produced by the HF (45% energy from fat) diet is milder, begins in the liver and progresses to peripheral tissues more slowly than with very-HF diets (55–60% of energy from fat). For example, male Wistar and Sprague Dawley rats consuming a diet with 59% of energy from fat developed hepatic but not muscle insulin resistance after 3 days [2,32]. However, after 3 weeks, insulin resistance had spread from the liver to other peripheral tissues [32]. With the more physiologically relevant level of fat used in the present studies (45% of energy from fat), insulin resistance did not progress beyond the liver during the 3–8 week study period.

The initiation of insulin resistance in specific tissues becomes physiologically important when the pancreas compensates for whole-body insulin resistance and increases insulin release. For example, the rapid increase in fat deposition between 3 and 8 weeks coincides with the time frame when hyperinsulinaemia became evident in our HF group [13]. Using independent methods in separate cohorts, we showed that adipose tissue was fully responsive to insulin during this period. Given the important lipogenic and anti-lipolytic roles of insulin in adipose tissue, our findings suggest that hepatic insulin resistance in conjunction with retention of peripheral insulin sensitivity created conditions that accentuated fat deposition in adipose tissue. This response may be a mechanism to prevent or delay ectopic fat accumulation and may also explain the slower progression of insulin resistance to peripheral tissues with the HF (45% of energy from fat) diet [2–4,32–34].

The precise mechanisms initiating diet-induced insulin resistance among peripheral tissues remain poorly understood. Although it is generally accepted that ectopic lipid accumulation is closely tied to insulin resistance [20,25,35], the identity of the accumulated lipids and underlying mechanism(s) that compromise insulin signalling remain uncertain [29,30]. It is also not clear whether the same lipid metabolites are responsible for producing insulin resistance among all tissues. For example, various lines of evidence suggest that accumulation of fatty acyl-CoAs compromises insulin signalling in muscle and liver [36–38], but recent evidence supports a specific causative role for increased short-chain fatty acylcarnitines in muscle [28,30]. In our studies, short-chain acylcarnitines were unaltered in muscle of the HF groups, with the tissue retaining full responsiveness to insulin despite higher levels of triacylglycerol and long-chain acylcarnitines. In contrast, the hepatic acylcarnitine profiles suggested enhanced long-chain fatty acid catabolism in the HF groups and accumulation of short- and medium-chain fatty acid metabolites. It is unclear whether the accumulation of short-chain fatty acylcarnitines caused hepatic insulin resistance through a mechanism similar to that reported in muscle by Koves et al. [28,29]. It is also possible that the altered hepatic acylcarnitine profiles were merely secondary to the insulin resistance produced in liver by the

HF diets and reflect loss of metabolic flexibility. Recent studies have shown that systemic glucose homeostasis and endogenous glucose production are rapidly regulated through hypothalamic lipid sensing mechanisms [39,40]. These findings illustrate that other signalling inputs may be altered by the HF diet and subsequently modifying insulin's ability to regulate endogenous glucose production.

Recent work from our laboratory established that dietary quercetin provided as a 1% food admixture reduced circulating markers of inflammation in mice on the HF (45% of energy from fat) diet [13]. This prompted a more rigorous evaluation of the response, with special emphasis on whether the flavonoid would also ameliorate progression of diet-induced insulin resistance. We hypothesised that quercetin might have protective effects, if reactive oxygen species are an underlying mediator of the insulin resistance produced by ectopic lipid accumulation and the predicted mitochondrial stress [29]. Our prediction is supported by a recent report showing significant reductions in insulin resistance, hyperlipidaemia and inflammation after oral administration of quercetin to fatty Zucker rats [14]. Previous studies with quercetin [41,42] reported beneficial effects from a wide range of doses (50 μg mouse^{-1} day^{-1} to 50 mg mouse^{-1} day^{-1}), so it was particularly surprising to find that dietary quercetin (0.8% wt/wt) exacerbated diet-induced insulin resistance at 3 weeks in our studies. By 8 weeks, the insulin resistance of the quercetin-supplemented group was no worse than in animals on HF diet alone. A composite evaluation of quercetin content and stability in the diet, intake and serum suggested that quercetin had an inhibitory effect on insulin signalling at 3 weeks that was eliminated by an adaptive increase in hepatic metabolism [43] and/or excretion of the compound between 3 and 8 weeks. Quercetin is an effective inhibitor of PI-3K and phospholipase A2 with an IC$_{50}$ of 3.8 μmol/l [44,45]. Given the relative permeability of hepatocytes to small molecules and the effectiveness of quercetin as an inhibitor of PI-3K and phospholipase A2, it seems likely that the concentration range of serum quercetin at 3 weeks (24–36 μmol/l) was sufficient to inhibit insulin-dependent activation of PI-3K and exacerbate insulin resistance. Notwithstanding the reduction in inflammatory cytokines observed with this high dose [13], the beneficial effects of significantly lower doses of quercetin in genetic models of insulin resistance [14] and atherosclerosis [41] make a compelling case for identifying lower doses that retain most if not all of these beneficial effects. It will be important in future studies to determine the site(s) of action and whether the beneficial effects of quercetin are mediated through a common mechanism.

Supplementary Material

Refer to Web version on PubMed Central for supplementary material.

Acknowledgments

Abbreviations

Endo R_a

Endogenous hepatic glucose production

GIR

Glucose infusion rate

HF

High-fat

HF+Q

HF+quercetin

LF

Low-fat

PI-3K

Phosphoinositol 3-kinase

References

1. Surwit RS, Kuhn CM, Cochrane C, McCubbin JA, Feinglos MN. Diet-induced type II diabetes in C57BL/6J mice. Diabetes 1988;37:1163–1167. [PubMed: 3044882]

2. Kraegen EW, Clark PW, Jenkins AB, Daley EA, Chisholm DJ, Storlien LH. Development of muscle insulin resistance after liver insulin resistance in high-fat-fed rats. Diabetes 1991;40:1397–1403. [PubMed: 1936601]

3. Storlien LH, James DE, Burleigh KM, Chisholm DJ, Kraegen EW. Fat feeding causes widespread in vivo insulin resistance, decreased energy expenditure, and obesity in rats. Am J Physiol 1986;251:E576–E583. [PubMed: 3535532]

4. Park SY, Cho YR, Kim HJ, et al. Unraveling the temporal pattern of diet-induced insulin resistance in individual organs and cardiac dysfunction in C57BL/6 mice. Diabetes 2005;54:3530–3540. [PubMed: 16306372]

5. Watson PM, Commins SP, Beiler RJ, Hatcher HC, Gettys TW. Differential regulation of leptin release and function in A/J versus C57BL/6J mice during diet-induced obesity. Am J Physiol 2000;279:E356–E365.

6. de Wilde J, Mohren R, van den Berg S, et al. Short-term high fat-feeding results in morphological and metabolic adaptations in the skeletal muscle of C57BL/6J mice. Physiol Genomics 2008;32:360–369. [PubMed: 18042831]

7. Kay CD, Holub BJ. The effect of wild blueberry (*Vaccinium angustifolium*) consumption on postprandial serum antioxidant status in human subjects. Br J Nutr 2002;88:389–398. [PubMed: 12323088]

8. Knekt P, Kumpulainen J, Jarvinen R, et al. Flavonoid intake and risk of chronic diseases. Am J Clin Nutr 2002;76:560–568. [PubMed: 12198000]

9. Meyers KJ, Rudolf JL, Mitchell AE. Influence of dietary quercetin on glutathione redox status in mice. J Agric Food Chem 2008;56:830–836. [PubMed: 18198829]

10. Franco JL, Braga HC, Stringari J, et al. Mercurial-induced hydrogen peroxide generation in mouse brain mitochondria: protective effects of quercetin. Chem Res Toxicol 2007;20:1919–1926. [PubMed: 17944542]

11. Chow JM, Shen SC, Huan SK, Lin HY, Chen YC. Quercetin, but not rutin and quercitrin, prevention of H2O2-induced apoptosis via anti-oxidant activity and heme oxygenase 1 gene expression in macrophages. Biochem Pharmacol 2005;69:1839–1851. [PubMed: 15876423]

12. Park C, So HS, Shin CH, et al. Quercetin protects the hydrogen peroxide-induced apoptosis via inhibition of mitochondrial dysfunction in H9c2 cardiomyoblast cells. Biochem Pharmacol 2003;66:1287–1295. [PubMed: 14505808]

13. Stewart LK, Soileau JL, Ribnicky D, et al. Quercetin transiently increases energy expenditure but persistently decreases circulating markers of inflammation in C57BL/6J mice fed a high-fat diet. Metab Clin Exp 2008;57:S39–S46. [PubMed: 18555853]

14. Rivera L, Moron R, Sanchez M, Zarzuelo A, Galisteo M. Quercetin ameliorates metabolic syndrome and improves the inflammatory status in obese Zucker rats. Obesity (Silver Spring) 2008;16:2081–2087. [PubMed: 18551111]

15. Lowell BB, Shulman GI. Mitochondrial dysfunction and type 2 diabetes. Science 2005;307:384–387. [PubMed: 15662004]

16. Savage DB, Petersen KF, Shulman GI. Disordered lipid metabolism and the pathogenesis of insulin resistance. Physiol Rev 2007;87:507–520. [PubMed: 17429039]

17. Houstis N, Rosen ED, Lander ES. Reactive oxygen species have a causal role in multiple forms of insulin resistance. Nature 2006;440:944–948. [PubMed: 16612386]

18. Hotamisligil GS. Inflammation and metabolic disorders. Nature 2006;444:860–867. [PubMed: 17167474]

19. Baukal AJ, Hunyady L, Catt KJ, Balla T. Evidence for participation of calcineurin in potentiation of agonist-stimulated cyclic AMP formation by the calcium-mobilizing hormone, angiotensin II. J Biol Chem 1994;269:24546–24549. [PubMed: 7929124]

20. Hegarty BD, Furler SM, Ye J, Cooney GJ, Kraegen EW. The role of intramuscular lipid in insulin resistance. Acta Physiol Scand 2003;178:373–383. [PubMed: 12864742]

21. An J, Muoio DM, Shiota M, et al. Hepatic expression of malonyl-CoA decarboxylase reverses muscle, liver and whole-animal insulin resistance. Nat Med 2004;10:268–274. [PubMed: 14770177]

22. Ayala JE, Bracy DP, McGuinness OP, Wasserman DH. Considerations in the design of hyperinsulinemic-euglycemic clamps in the conscious mouse. Diabetes 2006;55:390–397. [PubMed: 16443772]

23. Goodyear LJ, Giorgino F, Sherman LA, Carey J, Smith RJ, Dohm GL. Insulin receptor phosphorylation, insulin receptor substrate-1 phosphorylation, and phosphatidylinositol 3-kinase activity are decreased in intact skeletal muscle strips from obese subjects. J Clin Invest 1995;95:2195–2204. [PubMed: 7537758]

24. Gettys TW, Ramkumar V, Uhing RJ, Seger L, Taylor IL. Alterations in mRNA levels, expression, and function of GTP-binding regulatory proteins in adipocytes from obese mice (C57BL/6J-*ob/ob*). J Biol Chem 1991;266:15949–15955. [PubMed: 1908462]

25. Bonen A, Parolin ML, Steinberg GR, et al. Triacylglycerol accumulation in human obesity and type 2 diabetes is associated with increased rates of skeletal muscle fatty acid transport and increased sarcolemmal FAT/CD36. FASEB J 2004;18:1144–1146. [PubMed: 15132977]

26. Lee Y, Hirose H, Ohneda M, Johnson JH, McGarry JD, Unger RH. β-cell lipotoxicity in the pathogenesis of non-insulin-dependent diabetes mellitus of obese rats: Impairment in adipocyte- β-cell relationships. Proc Natl Acad Sci USA 1994;91:10878–10882. [PubMed: 7971976]

27. Hegarty BD, Cooney GJ, Kraegen EW, Furler SM. Increased efficiency of fatty acid uptake contributes to lipid accumulation in skeletal muscle of high fat-fed insulin-resistant rats. Diabetes 2002;51:1477–1484. [PubMed: 11978645]

28. Koves TR, Li P, An J, et al. PPARgamma coactivator-1alpha-mediated metabolic remodeling of skeletal myocytes mimics exercise training and reverses lipid-induced mitochondrial inefficiency. J Biol Chem 2005;280:33588–33598. [PubMed: 16079133]

29. Koves TR, Ussher JR, Noland RC, et al. Mitochondrial overload and incomplete fatty acid oxidation contribute to skeletal muscle insulin resistance. Cell Metab 2008;7:45–56. [PubMed: 18177724]

30. Bouzakri K, Austin R, Rune A, et al. Malonyl coenzymeA decarboxylase regulates lipid and glucose metabolism in human skeletal muscle. Diabetes 2008;57:1508–1516. [PubMed: 18314420]

31. Neschen S, Morino K, Hammond LE, et al. Prevention of hepatic steatosis and hepatic insulin resistance in mitochondrial acyl-CoA:glycerol-sn-3-phosphate acyltransferase 1 knockout mice. Cell Metab 2005;2:55–65. [PubMed: 16054099]

32. Samuel VT, Liu ZX, Qu X, et al. Mechanism of hepatic insulin resistance in non-alcoholic fatty liver disease. J Biol Chem 2004;279:32345–32353. [PubMed: 15166226]

33. Commerford SR, Bizeau ME, McRae H, Jampolis A, Thresher JS, Pagliassotti MJ. Hyperglycemia compensates for diet-induced insulin resistance in liver and skeletal muscle of rats. Am J Physiol 2001;281:R1380–R1389.

34. Pagliassotti MJ, Horton TJ, Gayles EC, Koppenhafer TA, Rosenzweig TD, Hill JO. Reduced insulin suppression of glucose appearance is related to susceptibility to dietary obesity in rats. Am J Physiol 1997;272:R1264–R1270. [PubMed: 9140029]

35. Rasouli N, Molavi B, Elbein SC, Kern PA. Ectopic fat accumulation and metabolic syndrome. Diabetes Obes Metab 2007;9:1–10. [PubMed: 17199713]

36. Pagliassotti MJ, Prach PA, Koppenhafer TA, Pan DA. Changes in insulin action, triglycerides, and lipid composition during sucrose feeding in rats. Am J Physiol 1996;271:R1319–R1326. [PubMed: 8945970]

37. Kim JK, Gavrilova O, Chen Y, Reitman ML, Shulman GI. Mechanism of insulin resistance in A-ZIP/F-1 fatless mice. J Biol Chem 2000;275:8456–8460. [PubMed: 10722680]

38. Yu C, Chen Y, Cline G, et al. Mechanism by which fatty acids inhibit insulin activation of insulin receptor substrate-1 (IRS-1)-associated phosphatidylinositol 3-kinase activity in muscle. J Biol Chem 2002;277:50230–50236. [PubMed: 12006582]

39. Obici S, Feng Z, Morgan K, Stein D, Karkanias G, Rossetti L. Central administration of oleic acid inhibits glucose production and food intake. Diabetes 2002;51:271–275. [PubMed: 11812732]

40. Pocai A, Obici S, Schwartz GJ, Rossetti L. A brain–liver circuit regulates glucose homeostasis. Cell Metab 2005;1:53–61. [PubMed: 16054044]

41. Hayek T, Fuhrman B, Vaya J, et al. Reduced progression of atherosclerosis in apolipoprotein E-deficient mice following consumption of red wine, or its polyphenols quercetin or catechin, is associated with reduced susceptibility of LDL to oxidation and aggregation. Arterioscler Thromb Vasc Biol 1997;17:2744–2752. [PubMed: 9409251]

42. da Silva J, Herrmann SM, Heuser V, et al. Evaluation of the genotoxic effect of rutin and quercetin by comet assay and micronucleus test. Food Chem Toxicol 2002;40:941–947. [PubMed: 12065216]

43. Lesser S, Cermak R, Wolffram S. The fatty acid pattern of dietary fat influences the oral bioavailability of the flavonol quercetin in pigs. Br J Nutr 2006;96:1047–1052. [PubMed: 17181879]

44. Matter WF, Brown RF, Vlahos CJ. The inhibition of phosphatidylinositol 3-kinase by quercetin and analogs. Biochem Biophys Res Commun 1992;186:624–631. [PubMed: 1323287]

45. Lindahl M, Tagesson C. Selective inhibition of group II phospholipase A2 by quercetin. Inflammation 1993;17:573–582. [PubMed: 8225564]
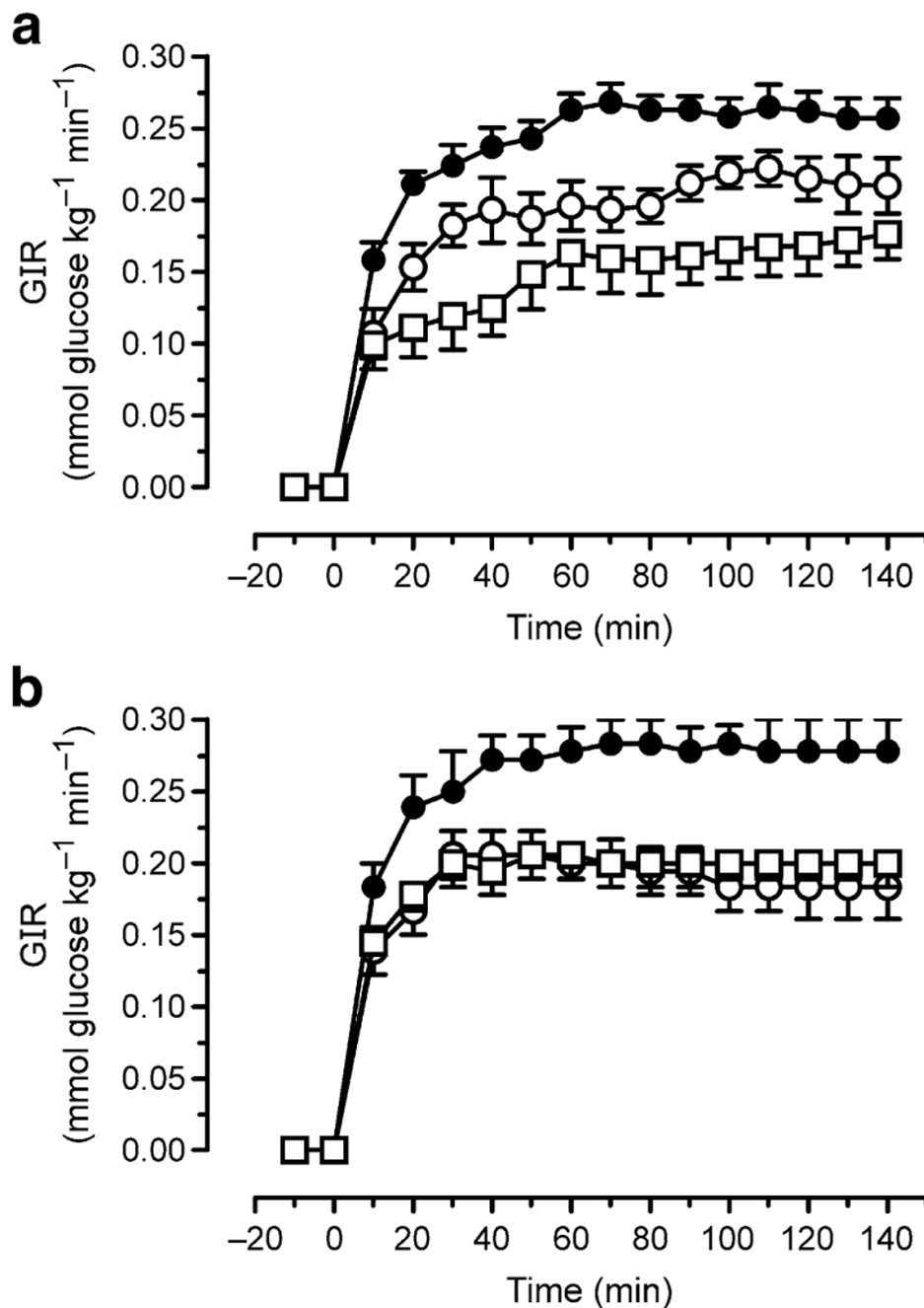
Fig. 1.
GIR (mean±SEM) required to maintain euglycaemia during hyperinsulinaemic clamp after 3 (**a**) or 8 (**b**) weeks on LF (black circles), HF (white circles) or HF+Q (white squares) diets. The clamp procedures were conducted with eight to ten mice per diet after 3 and 8 weeks on the respective diets. The steady-state clamp GIRs were compared by ANOVA as described in the Methods section and were lower ($p<0.05$) in mice on HF vs LF diet at 3 (**a**) and at 8 (**b**) weeks. The addition of quercetin to the HF diet further reduced GIR compared with HF alone at 3 weeks ($p<0.05$), but had no additional effect beyond that of HF at 8 weeks (**b**)
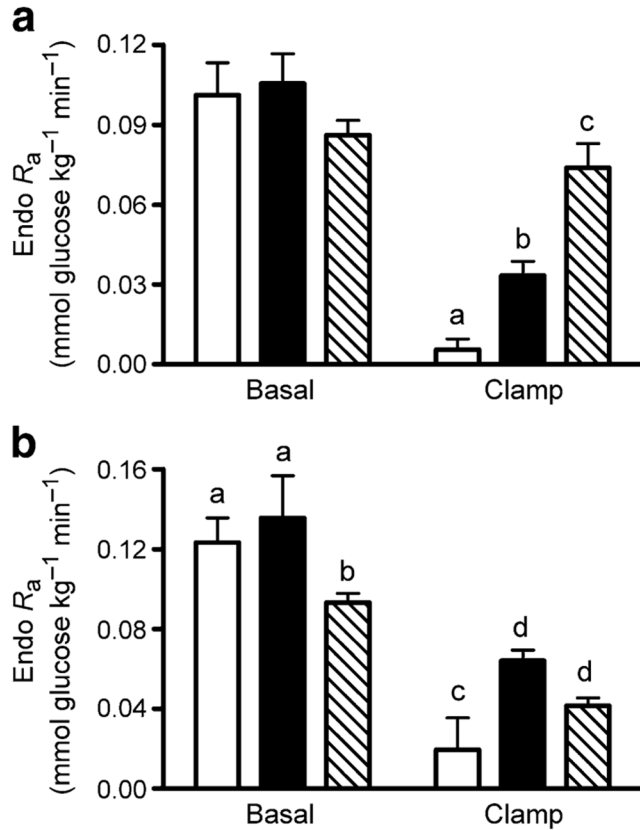
Fig. 2.
Rates (mean±SEM) of Endo R_a prior to and during hyperinsulinaemic clamp after 3 (**a**) or 8 (**b**) weeks on LF (white bars), HF (black bars) or HF+Q (hatched bars) diets. The clamp procedures were conducted with eight to ten mice per diet after 3 and 8 weeks on the respective diets to test how effectively insulin suppressed Endo R_a. Basal Endo R_a did not differ among the groups at 3 weeks (**a**) but was lower in HF+Q vs LF and HF groups at 8 weeks (**b**). The HF diet compromised suppression of Endo R_a by insulin at 3 and 8 weeks. Quercetin exacerbated the effect of the HF diet at 3 (**a**) but not at 8 weeks (**b**). The rates of Endo R_a during the basal and clamp periods were compared by ANOVA as described in the Methods section. Within the basal or clamp periods, means denoted by different superscript letters were significantly different ($p<0.05$)
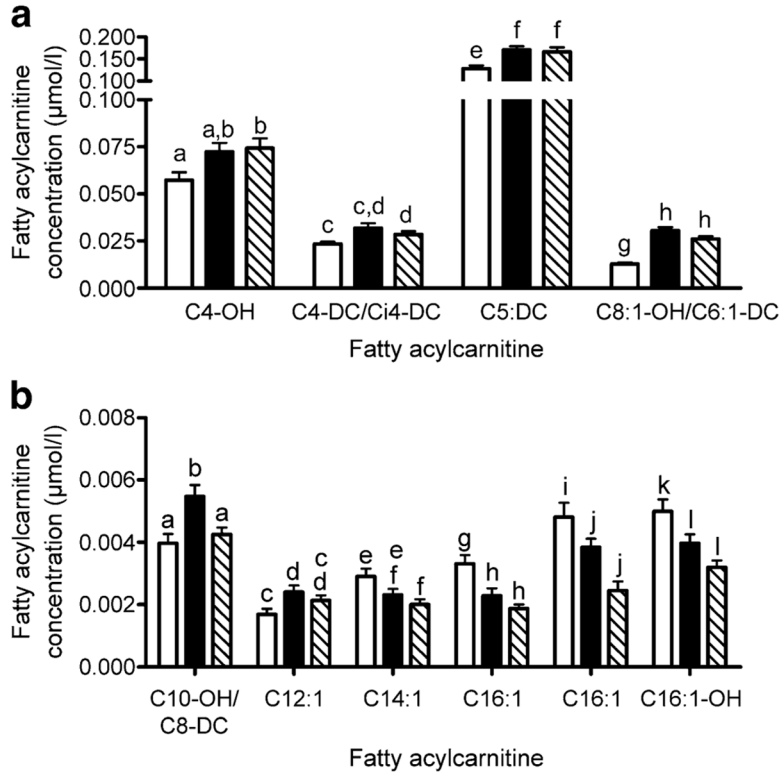
Fig. 3.
Fatty acylcarnitine profiles were obtained by tandem mass spectrometry in hepatic extracts from mice after consumption of LF (*n*=32; white bars), HF (*n*=32; black bars) or HF+Q (*n*=31; hatched bars) diets for 3 and 8 weeks. The effect of diet on short-chain (**a**) and long-chain (**b**) acylcarnitines was assessed by ANOVA as described in the Methods section. For each acylcarnitine subtype, means denoted by different superscripts letters were significantly different (*p*<0.05). C4-OH, 3-hydroxy-butyryl carnitine; C4-DC/Ci4-DC, succinyl carnitine or methylmalonyl carnitine; C5:DC, glutaryl carnitine; C8:1-OH/C6:1-DC, 3-hydroxy-*cis*-5-octenoyl carnitine or hexenedioyl carnitine; C10-OH/C8-DC, 3-hydroxy-decanoyl carnitine or hexenedioyl carnitine; C12:1, dodecenoyl carnitine; C14:1, tetradecadienoyl carnitine; C16:2, hexadecadienoyl carnitine; C16:1, palmitoleoyl carnitine; C16:1-OH, 3-hydroxy-palmitoleoyl carnitine
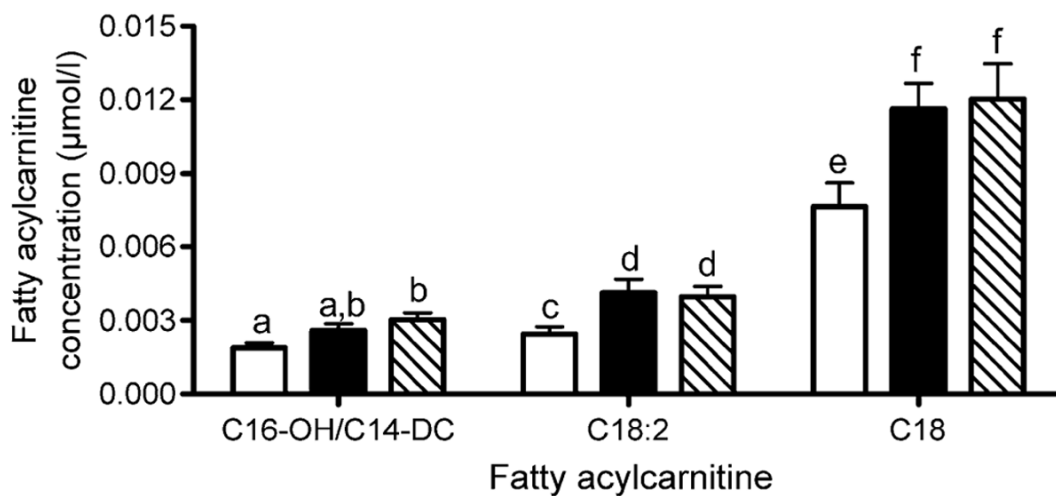
Fig. 4.
Fatty acylcarnitine profiles were obtained as in Fig. 3 in quadriceps muscle extracts from mice after consumption of the three diets for 8 weeks. LF, *n*=16; HF, *n*=16; HF+Q, *n*=16. The effect of diet on each acylcarnitine was tested by ANOVA as described in the Methods. Means denoted by different superscript letters were significantly different (*p*=0.05). C16-OH/C14-DC, 3-hydroxy-hexadecanoyl or tetradecanedioyl carnitine; C18:2, linoleyl carnitine; C18, Stearoyl carnitine
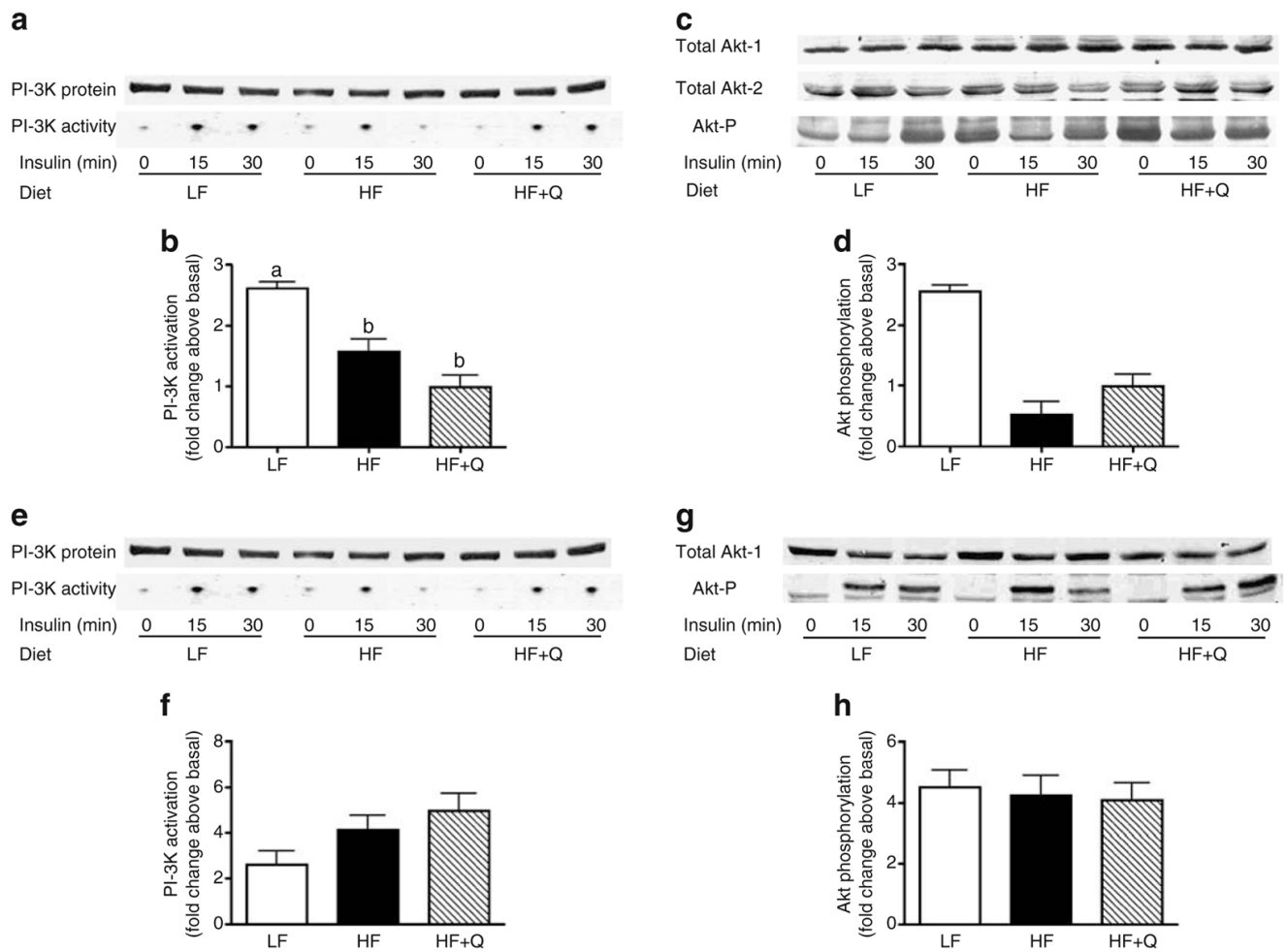
Fig. 5.
Insulin-dependent activation of PI-3K (**a**, **b**) and Akt (**c**, **d**) in hepatic extracts from mice after consumption of the three diets for 8 weeks. LF, *n*=8; HF, *n*=8; HF+Q, *n*=8. Insulin-dependent activation of PI-3K (**e**, **f**) and Akt (**g**, **h**) in muscle extracts from mice after diet as above. LF, *n*=4; HF, *n*=4; HF+Q, *n*=4. The mice were fasted for 8 h prior to killing at 0, 15 and 30 min after injection of insulin (5 U/kg body weight). PI-3K and Akt activity and expression were measured as described in Methods. Representative blots and activity measurements are shown. PI-3K activity and the increase in Akt-P were expressed as fold activation of PI-3K and Akt-P at 30 min relative to basal activity. Bar graphs show the means from three mice per time point per dietary group. The effect of diet on PI-3K activation and the increase in Akt-P were assessed by ANOVA. Means denoted by different superscript letters were significantly different (*p*<0.05)
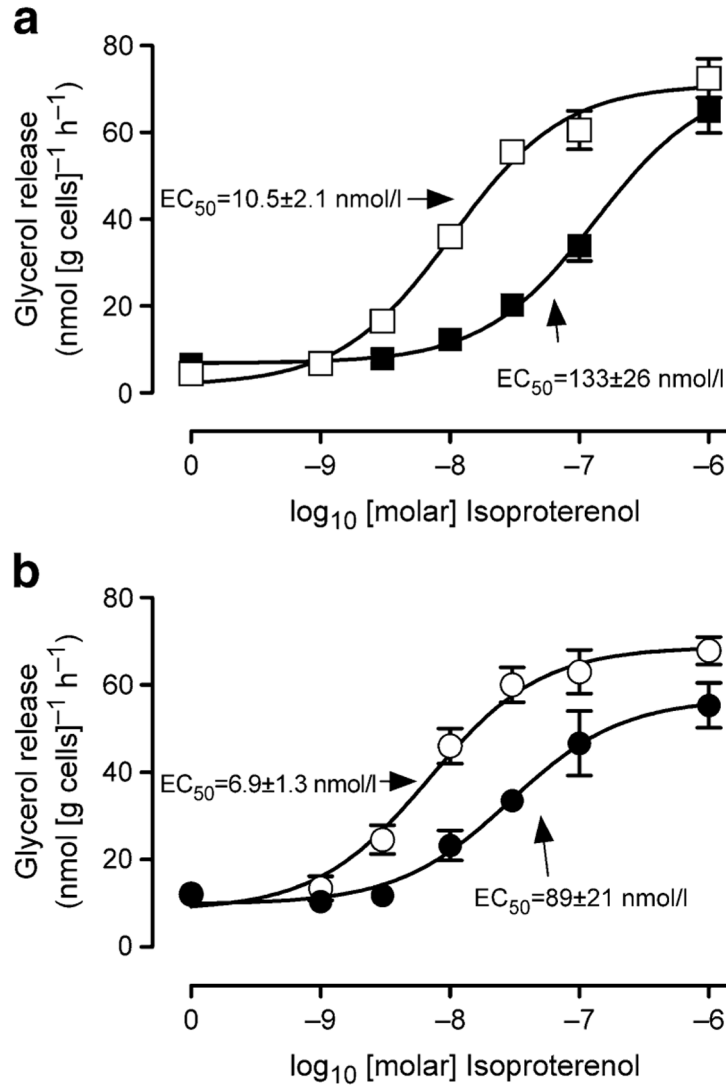
Fig. 6.
Inhibition of isoproterenol-dependent activation of lipolysis by insulin in adipocytes isolated from mice after consumption of LF (**a**) or HF (**b**) diets for 8 weeks. Epididymal white adipocytes were isolated from three mice per group after a 5 h fast and preincubated with 1 nmol/l insulin for 5 min prior to addition of half log increments of isoproterenol and further incubation for 1 h at 37°C in a shaking water-bath. Glycerol release into the medium was measured and representative dose–response curves from one of three replicates of the experiment are shown. Dose–response curves were fitted as described in the Methods section. Insulin sensitivity was assessed by comparing the change in EC_{50} of isoproterenol produced by insulin in adipocytes from the two dietary groups. White squares and circles, without insulin; black squares and circles, with insulin; EC_{50}, concentration of isoproterenol producing half maximal activation of glycerol release from cells

Table 1

Physical and laboratory variables in mice from cohorts 1 and 2, respectively

Variable	Week 0	Week 3			Week 8		
	LF	LF	HF	HF+Q	LF	HF	HF+Q
Body weight (g)	19.6±0.11	22.3±0.21	22.8±0.28	22.7±0.22	26.8±0.54[a]	28.9±0.62[b]	27.9±0.68[ab]
Food consumption (kJ per day)	–	10.2±0.21[a]	11.6±0.20[b]	11.0±0.21[a,b]	10.7±0.28[a]	11.5±0.36[b]	11.7±0.36[b]
Per cent fat mass (g fat [g body weight]$^{-1}$ ×100)	10.0±0.11	9.9±0.45[a]	11.9±0.43[b]	12.0±0.53[b]	14.5±0.91[a]	20.9±1.0[b]	20.7±1.4[b]
Blood glucose (mmol/l)	–	8.1±0.6	8.1±0.6	8.5±0.4	7.4±0.6	8.4±0.6	7.9±0.4
Plasma insulin (pmol/l)	–	241.4±34.5	189.7±17.2	224.1±34.5	172.4±17.2[a]	344.8±103.4[b]	137.9±17.24[a]
Plasma TG (mmol/l)	–	5.73±0.84[a]	8.37±0.92[a]	9.19±1.14[a]	5.76±1.61[a]	8.90±0.81[a]	6.4±1.35[a]
Plasma NEFA (mmol/l)	–	0.338±0.024[a]	0.396±0.031[a]	0.413±0.031[a]	0.318±0.028[a]	0.514±0.058[b]	0.402±0.054[a,b]
Muscle TG (μmol/g tissue)	–	4.28±0.49[a]	4.71±0.32[a]	6.23±0.66[a]	2.39±0.29[a]	4.99±0.55[b]	4.86±0.70[b]
Liver TG (μmol/g tissue)	–	5.74±1.15[a]	6.68±0.79[a]	6.44±2.26[a]	12.0±2.1[a]	16.4±2.3[a]	11.0±1.3[a]

Values are means±SEM

Measures were obtained from eight to ten mice per treatment group in each cohort

Fasting insulin and glucose concentrations (cohort 2) were measured at baseline, prior to the clamp procedure, after 3 or 8 weeks on LF, HF or HF+Q diets

For each variable, values with different superscripts letters within age (3 weeks or 8 weeks) were significantly different ($p<0.05$ by ANOVA) TG, triacylglycerol

Table 2

Mean rates of 2-deoxyl[^{3}H]glucose uptake (pmol glucose min^{-1} [mg tissue]$^{-1}$) among tissues during hyperinsulinaemic clamp after 3 or 8 weeks on LF, HF or HF+Q diets

Tissue	3 weeks LF (n=10)		3 weeks HF (n=9)		3 weeks HF+Q (n=10)		8 weeks LF (n=6)		8 weeks HF (n=6)		8 weeks HF+Q (n=7)	
	Mean	SEM	Mean	SEM	Mean	SEM	Mean	SEM	Mean	SEM	Mean	SEM
Soleus	0.560	0.091	0.621	0.073	0.652	0.177	0.707	0.365	0.627	0.183	0.548	0.079
Gastro	0.110	0.012	0.110	0.012	0.097	0.012	0.134	0.049	0.110	0.031	0.110	0.012
Vastus	0.097	0.006	0.134	0.024	0.085	0.018	0.116	0.043	0.079	0.018	0.097	0.012
Adipose	0.031	0.006	0.031	0.006	0.024	0.006	0.024	0.006	0.031	0.012	0.024	0.006
Diaphragm	0.920	0.079	1.030	0.128	1.097	0.238	0.822	0.177	0.804	0.116	0.865	0.134
Heart	3.392	0.420	2.741	0.432	2.594	0.493	2.875	0.445	2.351	0.566	1.912	0.530
Brain	0.451	0.043	0.402	0.018	0.420	0.037	0.317	0.067	0.378	0.067	0.378	0.043
Total R_d[a]	0.292	0.018	0.268	0.024	0.261	0.031	0.361	0.029	0.269	0.014	0.262	0.013
Plasma insulin	20.1	2.1	20.1	3.5	16.0	0.7	16.0	0.7	14.6	0.7	17.4	1.4

The clamp procedures were conducted with eight to ten mice per diet after 3 and 8 weeks on the respective diets.

The mean glucose uptake rates were compared by ANOVA as described in the Methods section

[a]The mean total glucose disposal rate (R_d) during the clamps was expressed as mmol glucose kg^{-1} min^{-1}; mean plasma insulin concentration during the clamps was expressed as pmol/l

Adipose, epididymal white adipose tissue; Soleus, soleus muscle; Gastro, gastrocnemius muscle; Vastus, vastus lateralis muscle